The role of trip lengths in control strategies and Macroscopic Fundamental Diagram traffic models

Sérgio F. A. Batista*[1], Deepak Ingole†[1], Ludovic Leclercq‡[1] and Monica Menendez§[2,3]

[1]Univ. Lyon, IFSTTAR, ENTPE, LICIT, F-69675, Lyon, France
[2]Division of Engineering, New York University Abu Dhabi, United Arab Emirates
[3]Tandon School of Engineering, New York University, USA

February 1, 2019

Words count: 1483 words

Introduction

Aggregated traffic models were introduced by Godfrey (1969) and later revisited by Daganzo (2007) and Geroliminis & Daganzo (2008). These traffic models require the partition of the city network (see e.g., Saeedmanesh & Geroliminis, 2016, 2017, Lopez et al., 2017, Casadei et al., 2018) into regions, where the traffic conditions are approximately homogeneous. Such partition defines the regional network. In each region, the traffic states are measured through the vehicles' accumulation $n(t)$ and are regulated by a Macroscopic Fundamental Diagram (MFD). The MFD reflects the relationship between the average circulating flow of vehicles and the average density in the region.

The regional network definition brings new challenges. Figure 1 depicts the challenge of scaling up trips to the regional network. The green and blue trips follow a sequence of links in the city network, with a fixed length. The green and blue trips cross a different sequence of regions, following the city network partitioning. The ordered sequence of crossed regions by a trip is called regional path. The green and blue trips describe different travel distances inside each region, as highlighted in the gray region. Therefore, regional paths are characterized by distributions of trip lengths, containing information of the plausible travel distances in the city

*✉ sergio.batista@ifsttar.fr
†✉ deepak.ingole@entpe.fr
‡✉ ludovic.leclercq@entpe.fr
§✉ monica.menendez@nyu.edu

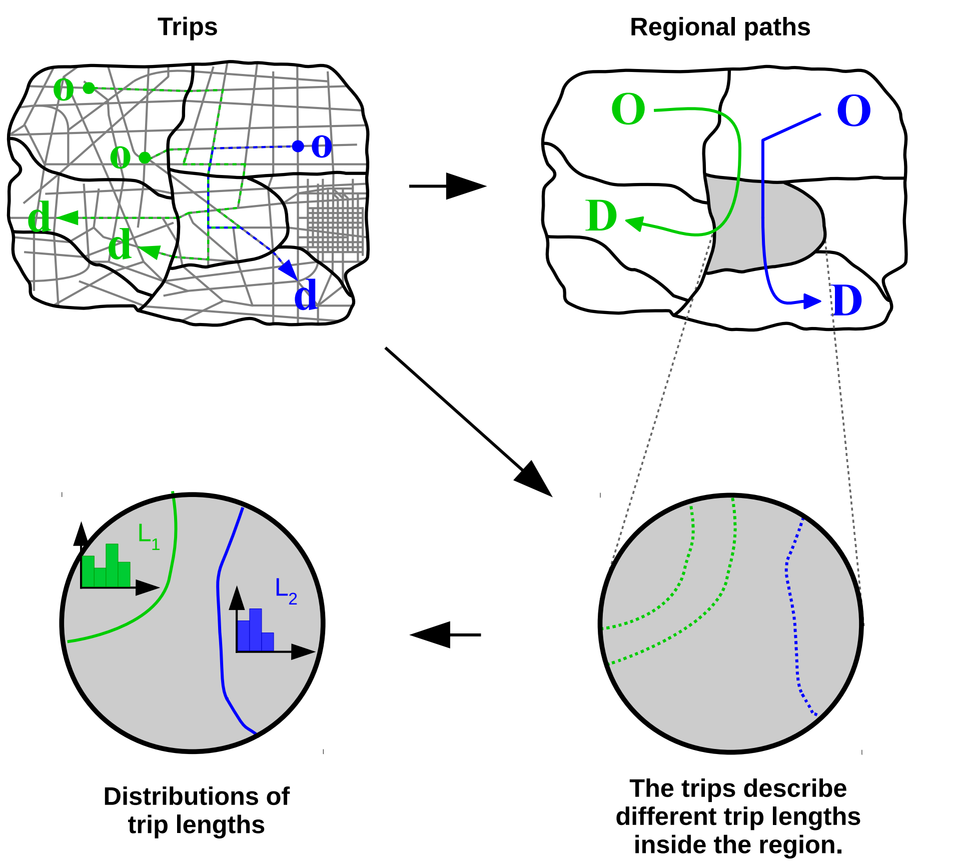

Fig. 1 – *The scale up of trips into regional paths, that are characterized by trip length distributions.*

network. Batista et al. (2018) and Batista et al. (in prep.) propose a methodological framework to calculate trip length distributions based on a set of trips and different levels of information from the regional network. The first level calculates trip length distributions considering the travel distances of all trips crossing one region. This assigns a common trip length distribution for all regional paths that cross the same region, independtly of their Origin and Destination (OD). We refer to this level as $M_{standard}$. The most detailed level only considers the trips that define the same regional path. This allows to derive different trip lengths for all regional paths that cross the same region. We refer to this level as $M_{reference}$. The authors show that $M_{standard}$ is not able to capture the trip lengths variability of all regional paths crossing the same region. Moreover, they also show that the calibration of the trip lenghts clearly influences the modeled traffic dynamics inside the regions.

Up to now, most of the MFD applications have been designed to test control algorithms or design perimeter control strategies. Daganzo (2007), Keyvan-Ekbatani et al. (2012) and Ekbatani et al. (2013) tested perimeter control strategies for a one region network, where all vehicles were assigned a common average travel distance. Some theoretical studies (see e.g., Haddad, 2017, Zhong et al., 2017, Yang et al., 2018) focused on the outflow-MFD application, where all vehicles were assigned the same trip length. Aboudolas & Geroliminis (2013) and Kouvelas et al. (2017) tested perimeter control strategies in real city networks, but an average trip length for all regions was also considered.

Research contribution

In this paper, we propose to investigate the role of the trip lengths calibration for perimeter control strategies. The goal is to quantify the effects of improper assumptions on the travel distances in the regions on Model Predictive Control (MPC) based control strategies. In this extended abstract, we discuss some initial and preliminary results obtained by a Proportional-Integral (PI) gating control scheme on a real network.

Test scenario and methodological framework

The test network is depicted in Figure 2 (a). It includes the 3^{rd} and 6^{th} districts of Lyon and the city of Villeurbarnne (France). The network has 3127 nodes and 3363 links and is divided into seven regions. Figure 2 (b) depicts the MFD functions. They were calculated by assuming a bi-parabolic shape to fit microscopic simulation data obtained from Symuvia (Leclercq, 2007).

The calculation of the trip lengths and regional paths are based on a virtual trips set in the city network. To gather this set, we randomly sample 3 million origin and destination nodes in the city network and calculate the shortest-path in distance between each of them. To obtain the regional paths, we filter all trips by the specific sequence of regions they cross. For each regional OD pair, the regional paths are ranked according to the number of trips they have associated. For our case study, we consider three OD pairs: 1-7; 4-2; and 6-4. To define the regional choice set for each OD pair, we gather the two regional paths with the largest number of trips associated. We calculate the trip lengths distributions following the $M_{standard}$ and $M_{reference}$ described in the Introduction (see also Batista et al., 2018, in prep., , for more details). The regional paths and demand assignment coefficients are listed in Table 1. The average trip lengths calculated by $M_{standard}$ and $M_{reference}$ are listed in Table 2. The demand scenarios for the three OD pairs are shown in Figure 2 (c). The traffic states are simulated through an accumulation-based MFD model (Daganzo, 2007, Geroliminis & Daganzo, 2008), for a total simulation period of $T = 20000$ seconds.

Our goal is to control the maximum vehicles' accumulation in region 3 (i.e. $(n_3(t))$). For this purpose, we designed a gating control composed by three PI controllers with an anti-windup scheme to track the desired set-point, i.e. $(n_3(t))$. Figure 3 depicts the PI-based gating control scheme that is implemented. The inflows of regional paths $1-3-5-7$ ($I_{3,1}$[1]), $4-3-2$ ($I_{3,2}$) and $6-5-3-4$ ($I_{3,3}$) are manipulated by the PI controller before entering region 3. The new inflows are $u_{3,1}(t)$, $u_{3,2}(t)$ and $u_{3,3}(t)$. The manipulation by the controller is done such that $n_3(t)$ is maintained at the set-point. The ouflows $(o_{3,1}, o_{3,2}, o_{3,3})$ will continue to the next regions in the sequence of the correspoding regional paths. In this example,

[1]The first subscript refers to the region that is being controlled. The second subscript refers to the regional paths will cross region 3.

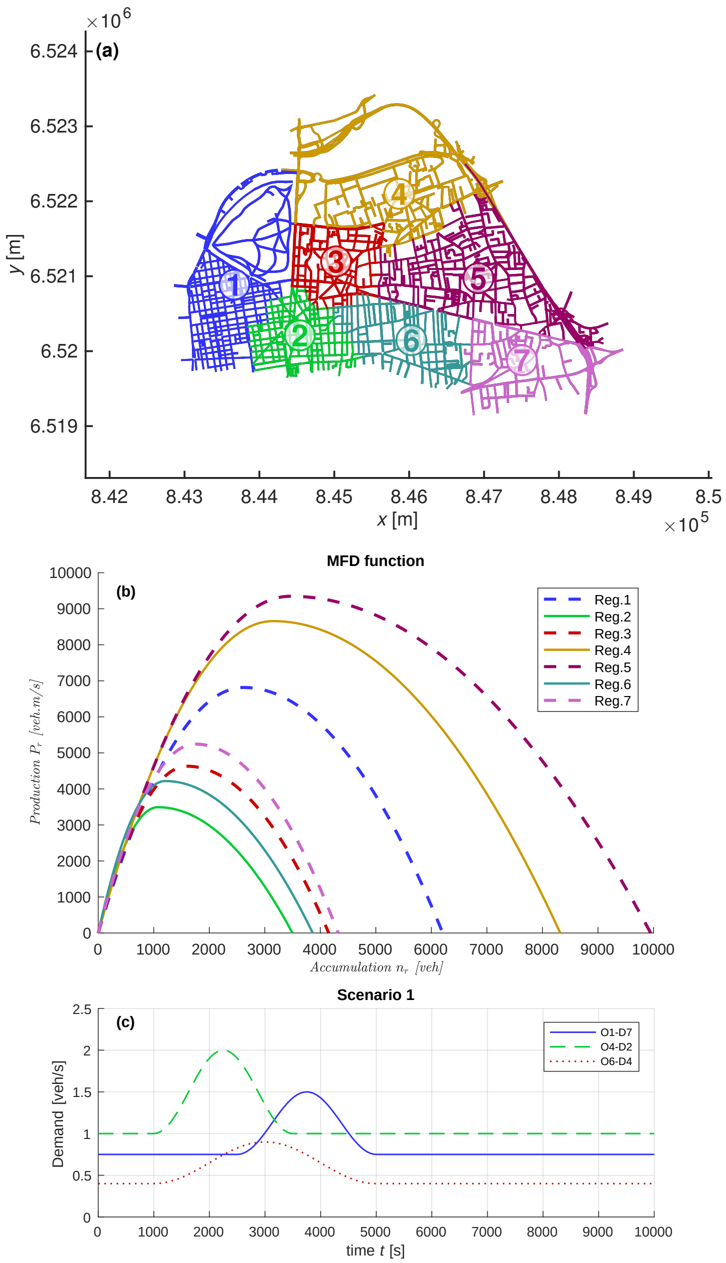

Fig. 2 – *(a) Villeurbarnne and the* 3^{rd} *and* 6^{th} *districts of Lyon (France) traffic network, divided into seven regions. (b) MFD function of each region. (c) Demand scenarios.*

O	D	Regional path	Assignment coefficient
1	7	1-2-6-7	0.15
		1-3-5-7	0.85
4	2	4-1-2	0.25
		4-3-2	0.75
6	4	4-3-2	0.00
		6-5-3-4	1.00

Tab. 1 – *Regional paths and the assignment coefficients used for this study.*

Method	Regional path	Region						
		1	2	3	4	5	6	7
Standard	1-2-6-7	987	649	∼	∼	∼	694	926
	1-3-5-7	987	∼	880	∼	1042	∼	926
	4-1-2	987	649	∼	1347	∼	∼	∼
	4-3-2	∼	649	880	1347	∼	∼	∼
	6-5-3-4	∼	∼	880	1347	1042	694	∼
Reference	1-2-6-7	788	1121	∼	∼	∼	1424	676
	1-3-5-7	927	∼	1297	∼	1032	∼	1142
	4-1-2	2761	335	∼	2227	∼	∼	∼
	4-3-2	∼	708	1049	1191	∼	∼	∼
	6-5-3-4	∼	∼	458	733	861	584	∼

Tab. 2 – *Average trip lengths (m) calculated by the methods* $M_{standard}$ *and* $M_{reference}$.

we assume that the set of regional paths and trip lengths remain unchanged. In the full paper, we will consider the vehicles' re-routing due to the control effects on the travel times and time-dependent trip lengths. The proportional ($k_p = 1$) and integral (($k_i = 0.05$)) gains of the PI controller are obtained using trial and error methods.

Preliminary results and discussion

Figure 4 depicts the evolution of the vehicles' accumulation $n(t)$ during the simulation period T, for all seven regions. We first briefly analyze the results for the uncontrolled cases, that are represented by the solid curves. We observe that the $n(t)$ peak between ∼3000-7000 seconds, is larger for the case of $M_{reference}$ compared to $M_{standard}$. This happens because the average trip lengths calculated through $M_{reference}$ for regional paths $1-2-6-7$ and $1-3-5-7$ are larger than the ones calculated through $M_{standard}$ (see Table 2). The speed-MFD is the same for all vehicles traveling in region 1. Therefore, they need more time to complete their

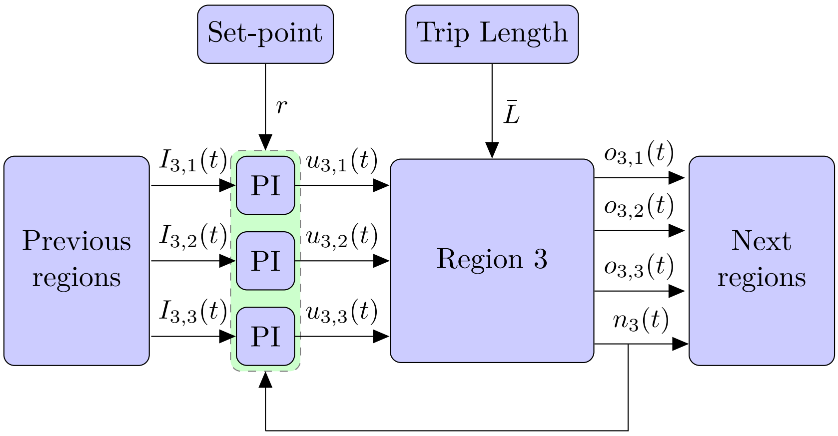

Fig. 3 – *Representation of closed-loop gating control using PI controllers.*

trips for $M_{reference}$ as the travel distance is longer, increasing the accumulation.

The results for the controlled cases are represented by the dashed lines. We are gating the inflow of the three regional paths that cross region 3 (see Table 1 for the list of these regional paths). When $n_3(t)$ reaches 500 vehicles, vehicles start queuing in regions 1, 4 and 5. These are the previous adjacent regions to 3 in the three regional path sequences. The vehicles' accumulation in these regions increases compared to the uncontrolled cases. This influences the traffic dynamics in the regions. This happens especially when the accumulation reaches the congestion branch of the MFD, where priority rules are applied.

Figure 2 (c) depicts one demand peak per OD pair, each happening at different time instants. From these three demand peaks, vehicles traveling on regional path $4-3-2$ are the first to arrive to region 3. They are allowed to enter region 3, until $n_3(t) = 500$ vehicles. The travel distances for region 3 assigned by $M_{reference}$ are larger than the ones by $M_{standard}$. Vehicles are then queuing for a longer period of time in region 4, for the case of $M_{reference}$ compared to $M_{standard}$. This leads to a larger accumulation for $M_{reference}$ than $M_{standard}$ in region 4. The next demand peaks to arrive are traveling on regional paths $6-5-4-3$ and $1-3-5-7$, respectively. Since region 3 is already at its maximum targeting accumulation, vehicles traveling on these two regional paths will be queuing in regions 5 and then 1. This leads to larger accumulations for these two regions for the case of $M_{reference}$ compared to $M_{standard}$.

These results highlight that the trip lengths calibration is very important and play an important role in the spreading of congestion to adjacent regions as well as on the regional traffic dynamics. In the full paper, we will analyse the role of the trip lengths estimation on the MPC.

Acknowledgments

This project is supported by the European Research Council (ERC) under the European Union's Horizon 2020 research and innovation program (grant agreement No 646592 - MAGnUM project).

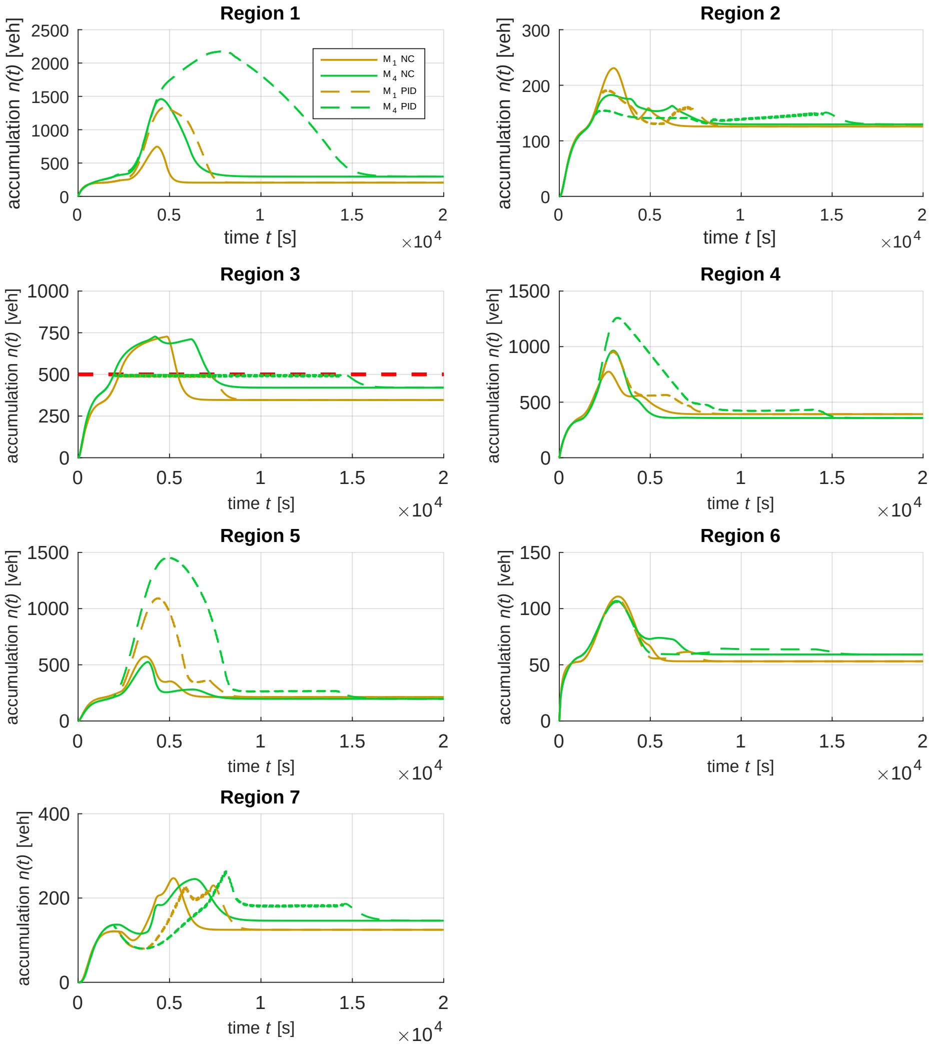

Fig. 4 – *Evolution of the vehicles' accumulation $n(t)$ for all seven regions.*

References

Aboudolas, K. & Geroliminis, N. (2013), *Perimeter and boundary flow control in multi-reservoir heterogeneous networks.* Transportation Research Part B: Methodological, 55, 265–281, doi:10.1016/j.trb.2013.07.003.

Batista, S. F. A., Leclercq, L. & Geroliminis, N. (in prep.), *Trip length estimation for the aggregated network models: scaling microscopic trips into reservoirs.*

Batista, S. F. A., Leclercq, L., Krug, J. & Geroliminis, N. (2018), *Trip length estimation for the macroscopic traffic simulation: scaling microscopic into macroscopic networks. In 97^{th} Annual Meeting Transportation Research Board*, Washington DC, USA.

Casadei, G., Bertrand, V., Gouin, B. & Canudas-de-Wit, C. (2018), *Aggregation and travel time calculation over large scale traffic networks: An empiric study on the grenoble city.* Transportation Research Part C: Emerging Technologies, 95, 713–730, doi:10.1016/j.trc.2018.07.033.

Daganzo, C. (2007), *Urban gridlock: Macroscopic modeling and mitigation approaches.* Transportation Research Part B: Methodological, 41, 49–62, doi:10.1016/j.trb.2006.03.001.

Ekbatani, M., Papageorgiou, M. & Papamichail, I. (2013), *Urban congestion gating control based on reduced operational network fundamental diagrams.* Transportation Research Part C: Emerging Technologies, 33, 74–87, doi:10.1016/j.trc.2013.04.010.

Geroliminis, N. & Daganzo, C. (2008), *Existence of urban-scale macroscopic fundamental diagrams: Some experimental findings.* Transportation Research Part B: Methodological, 42, 759–770, doi:10.1016/j.trb.2008.02.002.

Godfrey, J. W. (1969), *The mechanism of a road network.* Traffic Engineering and Control, 11, 323–327.

Haddad, J. (2017), *Optimal perimeter control synthesis for two urban regions with aggregate boundary queue dynamics.* Transportation Research Part B: Methodological, 96, 1–25, doi:10.1016/j.trb.2016.10.016.

Keyvan-Ekbatani, M., Kouvelas, A., Papamichail, I. & Papageorgiou, M. (2012), *Exploiting the fundamental diagram of urban networks for feedback-based gating.* Transportation Research Part B: Methodological, 46(10), 1393–1403, doi:10.1016/j.trb.2012.06.008.

Kouvelas, A., Saeedmanesh, M. & Geroliminis, N. (2017), *Enhancing model-based feedback perimeter control with data-driven online adaptive optimization.* Transportation Research Part B: Methodological, 96, 26–45, doi:10.1016/j.trb.2016.10.011.

Leclercq, L. (2007), *Hybrid approaches to the solutions of the "lighthill-whitham-richards" model.* Transportation Research Part B: Methodological, 41, 701–709, doi:10.1016/j.trb.2006.11.004.

Lopez, C., Leclercq, L., Krishnakumari, P., Chiabaut, N. & van Lint, H. (2017), *Revealing the day-to-day regularity of urban congestion patterns with 3d speed maps.* Scientific Reports, 7, 1–11, doi:10.1038/s41598-017-14237-8.

Saeedmanesh, M. & Geroliminis, N. (2016), *Clustering of heterogeneous networks with directional flows based on "snake" similarities.* Transportation Research Part B: Methodological, 91, 250–269, doi:10.1016/j.trb.2016.05.008.

Saeedmanesh, M. & Geroliminis, N. (2017), *Dynamic clustering and propagation of congestion in heterogeneously congested urban traffic networks.* Transportation Research Procedia, 23, 962–979, doi:10.1016/j.trb.2017.08.021.

Yang, K., Zheng, N. & Menendez, M. (2018), *Multi-scale perimeter control approach in a connected-vehicle environment.* Transportation Research Part C: Emerging Technologies, 94, 32–49, doi:10.1016/j.trc.2017.08.014.

Zhong, R., Chen, C., Huang, Y., Sumalee, A., Lam, W. & Xu, D. (2017), *Robust perimeter control for two urban regions with macroscopic fundamental diagrams: A control-lyapunov function approach.* Transportation Research Procedia, 23, 922–941, doi:10.3141/2493-09.